Talin activates integrins by altering the topology of the β transmembrane domain

Chungho Kim, Feng Ye, Xiaohui Hu, and Mark H. Ginsberg

Department of Medicine, University of California San Diego, La Jolla, CA 92093

Talin binding to integrin β tails increases ligand binding affinity (activation). Changes in β transmembrane domain (TMD) topology that disrupt α–β TMD interactions are proposed to mediate integrin activation. In this paper, we used membrane-embedded integrin β3 TMDs bearing environmentally sensitive fluorophores at inner or outer membrane water interfaces to monitor talin-induced β3 TMD motion in model membranes. Talin binding to the β3 cytoplasmic domain increased amino acid side chain embedding at the inner and outer borders of the β3 TMD, indicating altered topology of the β3 TMD. Talin's capacity to effect this change depended on its ability to bind to both the integrin β tail and the membrane. Introduction of a flexible hinge at the midpoint of the β3 TMD decoupled the talin-induced change in intracellular TMD topology from the extracellular side and blocked talin-induced activation of integrin αIIbβ3. Thus, we show that talin binding to the integrin β TMD alters the topology of the TMD, resulting in integrin activation.

Introduction

The separation of the intracellular and extracellular environments by plasma membranes is essential for most forms of life. At the same time, cells need to communicate information across membranes for functions such as migration, differentiation, multiplication, and survival (von Heijne and Rees, 2008). One form of transmembrane communication employs allosteric rearrangements in transmembrane proteins. Extracellular regions of such transmembrane proteins can sense signals from outside and transmit the signals to intracellular regions. Conversely, intracellular signaling events can influence behavior of the extracellular regions.

Integrins are composed of α and β subunits (Hynes, 2002; Shattil et al., 2010; Kim et al., 2011a) and mediate bidirectional transmembrane signaling. Intracellular signals lead to talin binding to cytoplasmic tails of integrin β subunits, thereby increasing the ligand binding affinity of the extracellular domain (operationally defined as activation), a process important in cell migration, ECM assembly, inflammation, and hemostasis (Tadokoro et al., 2003; Shattil et al., 2010). Binding of the talin head domain (THD) to the β3 cytoplasmic tail induces conformational changes in the extracellular domain of membrane-embedded αIIbβ3 integrin (Ye et al., 2010). As the integrin transmembrane domains (TMDs) link the cytoplasmic and extracellular domains of integrin β3, a change in the topology of the β TMD was proposed to mediate this transmembrane allostery (Williams et al., 1994).

The role of the topology of the integrin TMD has been the subject of conjecture for years (Williams et al., 1994; Li et al., 2002; Ginsberg et al., 2005), with changes in membrane tilt angle or pistonlike motions of the TMD into or out of the membrane suggested. Recent structural studies using integrin β cytoplasmic tail and THD (Wegener et al., 2007; Anthis et al., 2009) and molecular dynamic simulation (Kalli et al., 2010, 2011) added additional credence to the idea that talin binding may change tilt angle of integrin β TMD relative to the plane of the membrane. We recently showed that membrane embedding and therefore the tilt angle of the β3 TMD is required to maintain off-state α and β TMD interactions (Kim et al., 2011b), as was suggested by the structure of the αIIbβ3 TMD complex (Lau et al., 2009). The stability of the αIIbβ3 TMD interaction is required to maintain the integrin's low affinity state (Luo et al., 2004; Kim et al., 2009). Thus, the capacity of talin to change the membrane topology of the β TMD, thereby altering the α and β TMD interaction, may be crucial for integrin activation; however, to date, there has been no experimental assessment of the effect of talin on integrin TMD topology.

C. Kim and F. Ye contributed equally to this paper.

Correspondence to Mark H. Ginsberg: mhginsberg@ucsd.edu

Abbreviations used in this paper: KSI, ketosteroid isomerase; THD, talin head domain; TMD, transmembrane domain.

© 2012 Kim et al. This article is distributed under the terms of an Attribution–Noncommercial–Share Alike–No Mirror Sites license for the first six months after the publication date (see http://www.rupress.org/terms). After six months it is available under a Creative Commons License (Attribution–Noncommercial–Share Alike 3.0 Unported license, as described at http://creativecommons.org/licenses/by-nc-sa/3.0/).

The Rockefeller University Press $30.00
J. Cell Biol. Vol. 197 No. 5 605–611
www.jcb.org/cgi/doi/10.1083/jcb.201112141

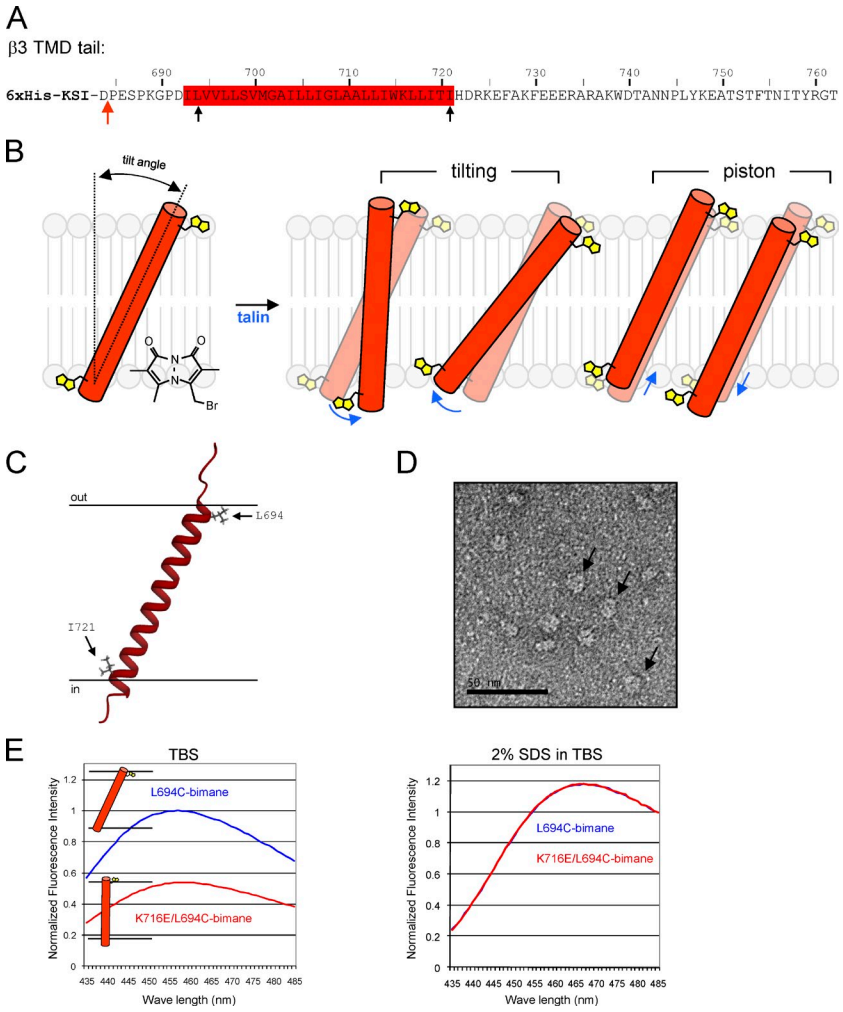

Figure 1. **Fluorescence-based assay for measuring TMD embedding.** (A) The amino acid sequence of β3 TMD tail peptide. The red arrow indicates the site of acid cleavage, and black arrows indicate bimane labeling sites. (B) Embedding changes of TMD. Yellow pentagons represent bimanes, and the structure of monobromobimane and TMD tilt angle are also shown. (C) Structure of β3 TMD, with side chains of Leu694 and Ile721 indicated. (D) Negative-stain electron microscopic image of nanodiscs containing β3 TMD tail peptide. Arrows indicate nanodiscs. Bar, 50 nm. (E) Emission spectra of nanodiscs containing β3 TMD tail bimane labeled at L694C (L694C-bimane nanodisc) in the presence or absence of K716E mutation (left). The same peptides in the presence of 2% SDS are shown on the right. Data are representative of three independent experiments.

Here, we used membrane-embedded integrin β3 TMDs bearing environmentally sensitive fluorophores at the inner or outer membrane water interfaces to monitor talin-induced β3 TMD movement in lipid bilayer. We report that THD binding to the β3 cytoplasmic domain increases the embedding of amino acid side chains at the inner and outer borders of the β3 TMD. Talin's capacity to effect this change depends on its capacity to bind to both the integrin β tail and the membrane. Introduction of a flexible hinge at the midpoint of the β3 TMD decouples the THD-induced change in intracellular TMD topology from the extracellular side and blocks THD-induced activation of integrin αIIbβ3. Thus, we show that talin binding to the integrin β TMD alters the topology of the TMD, resulting in destabilization of the α–β TMD complex and integrin activation.

Results and discussion

Talin increases the membrane embedding of the β3 TMD by binding to the β3 cytoplasmic tail

In principle, signals can be transmitted through movements of the TMD that include tilting or pistoning of the TMD (Fig. 1 B; Williams et al., 1994). As the β3 TMD is tilted by ∼25° relative to the normal axis of the membrane (Fig. 1 A; Lau et al., 2008), we reasoned that movements of the β3 TMD upon talin binding would lead to changes in the lipid embedding of the termini of the TMD (Fig. 1 B). We used bimane, an environment-sensitive fluorophore, to assess the hydrophobicity of the environment of the TMD termini (Fig. 1 B). Hydrophobicity gradually increases from the aqueous phase to the center of lipid bilayer (Subczynski et al., 1998); therefore, reduced tilting, as shown in Fig. 1 B, places both ends into a more hydrophilic environment, whereas increased tilting places them into a more hydrophobic environment. Similarly, an upward piston movement would place the N-terminal end into a more hydrophilic environment and the C-terminal end to a more hydrophobic environment, and downward pistoning would have the opposite effect. Bimane fluorescence emission increases with the increased hydrophobicity of the environment (Yao et al., 2006), as confirmed in solvents of progressively lower polarity (Fig. S1).

To monitor the relative embedding of the β3 TMD ends in the lipid bilayer, we purified β3 TMD cytoplasmic tail (TMD tail) peptides (Fig. 1 A) with Cys mutations either at Leu694 or Ile721 (Fig. 1 C) and labeled the Cys with bimane (Kosower et al., 1979). The peptide was then inserted into a nanodisc, a disc-shaped lipid bilayer encircled by membrane scaffold proteins derived from apolipoprotein A1 (Denisov et al., 2004). The nanodiscs were separated from free peptide by gel filtration, and

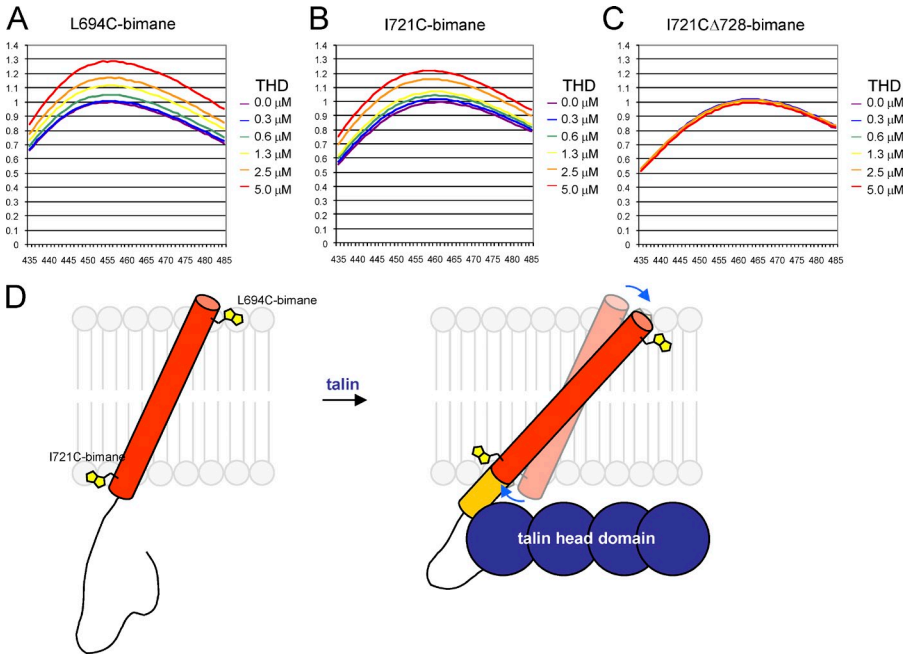

Figure 2. **Talin induces increased embedding of both ends of the β3 TMD.** (A) Emission spectra of L694C-bimane nanodisc in the presence of increasing concentrations of THD. Fluorescence intensities were normalized to the maximum fluorescence intensity when no THD was present. (B) The emission spectra of I721C-bimane nanodiscs were analyzed as in A. (C) Nanodiscs containing truncated β3 TMD tail peptide were bimane labeled at I721C (ΔI721C-bimane), and response to THD was analyzed as in A. (A–C) All data are representative of at least three independent experiments. (D) Talin-induced topographic change of β3 TMD that can account for altered embedding. Orange cylinders indicate a β3 cytoplasmic tail, which forms a stable helix upon talin binding.

successful assembly was confirmed by negatively stained electron micrographs (Fig. 1 D). To test whether we could detect changes in tilt angle, we compared the emission spectrum from the nanodisc containing wild-type β3 and β3(K716E) TMD tail peptide labeled with bimane at the L694C position. The β3(K716E) mutation decreases the β3 TMD tilt angle by removing a snorkeling Lys residue (Kim et al., 2011b); consequently, β3(K716E) would place the bimane conjugated to the side chain of Cys694 into a more hydrophilic environment (Fig. 1 C). As expected, the fluorescence of β3(L694C-bimane) was reduced by the K716E mutation (Fig. 1 E, left). This change depended on lipid embedding of the TMD because solubilizing the nanodiscs in 2% SDS (Fig. 1 E, right) resulted in similar emission spectra of β3(L694C) and β3(K716E,L694C) constructs.

Having established the validity of this approach, we examined the effect of the integrin-activating THD on the embedding of the β3 TMD by monitoring the changes in the emission spectrum of fluorophores placed at the N-terminal side of the TMD (Leu694) or C-terminal side (Ile721; Fig. 1 A). Addition of purified THD to L694C-bimane nanodisc increased the fluorescence intensity in a concentration-dependent manner; thus, talin binding caused a repositioning of an amino acid side chain at the β3 TMD N-terminal end to a more hydrophobic environment (Fig. 2 A). THD also increased the fluorescence intensity of I721C-bimane nanodisc (Fig. 2 B). This increase in fluorescence is a specific result of THD–β3 cytoplasmic tail interaction, as THD had no effect on the emission spectrum of a nanodisc containing β3(Δ728/I721C-bimane) peptide, which lacks the primary talin binding site (Tadokoro et al., 2003), as a result of the truncation of the β3 cytoplasmic tail (Fig. 2 C). Thus, THD binding to the β3 cytoplasmic tail causes side chains at both the N- and C-terminal end of β3 TMD to reside in more hydrophobic environments. The change of hydrophobicity from water to hydrophobic core of the membrane is not linear, and initial embedding of Ile721 and Leu694 differ; the relative embedding changes of those two residues are not directly comparable from the change in fluorescence. Thus, THD can induce changes in the topology of the β3 TMD compatible with increased tilt angle. That said, rotation and/or pistoning could also contribute to the changes we observed; however, pistoning would cause opposing effects on the two TMD termini (Fig. 1 B) and can therefore be excluded as the major effect of talin on the topology of the β3 TMD (Fig. 2 D).

A flexible kink blocks the transmission of talin-induced topological change to the extracellular side of the β3 TMD

We reasoned that transmission of a change induced by THD at the cytoplasmic (C terminal) end of the TMD would depend on a rigid helix connecting it to the extracellular (N terminal) end of the TMD. Pro in the middle of α helix is known to introduce a flexible kink as a result of its cyclic side chain that prohibits the helix-stabilizing hydrogen bond formation with the backbone of the preceding turn (Sansom and Weinstein, 2000; Cordes et al., 2002; Senes et al., 2004). Introduction of a Pro in the middle of the β3 transmembrane helix causes such a flexible kink (Kim et al., 2011b) that breaks the continuity of the TMD helix, partitioning it into N- and C-terminal helices. This kink would decouple the movement of the two ends of the TMD, resulting in blockade of transmission of altered topology across the membrane. We substituted Pro for Ala711 in β3 TMD tail peptides. In the absence of THD, we observed similar emission spectra between wild-type and A711P mutant peptides labeled with bimane in the L694C position (Fig. 3 A, purple lines). However, the A711P substitution relocated I721C-labeled bimane to a more hydrophilic environment (Fig. 3 B, purple lines), consistent with alteration of the topology of the C-terminal helix by introduction of a kink in the middle of the helix (Fig. 3 C, middle). More importantly, the A711P mutation markedly attenuated the capacity of THD to increase in fluorescence intensity

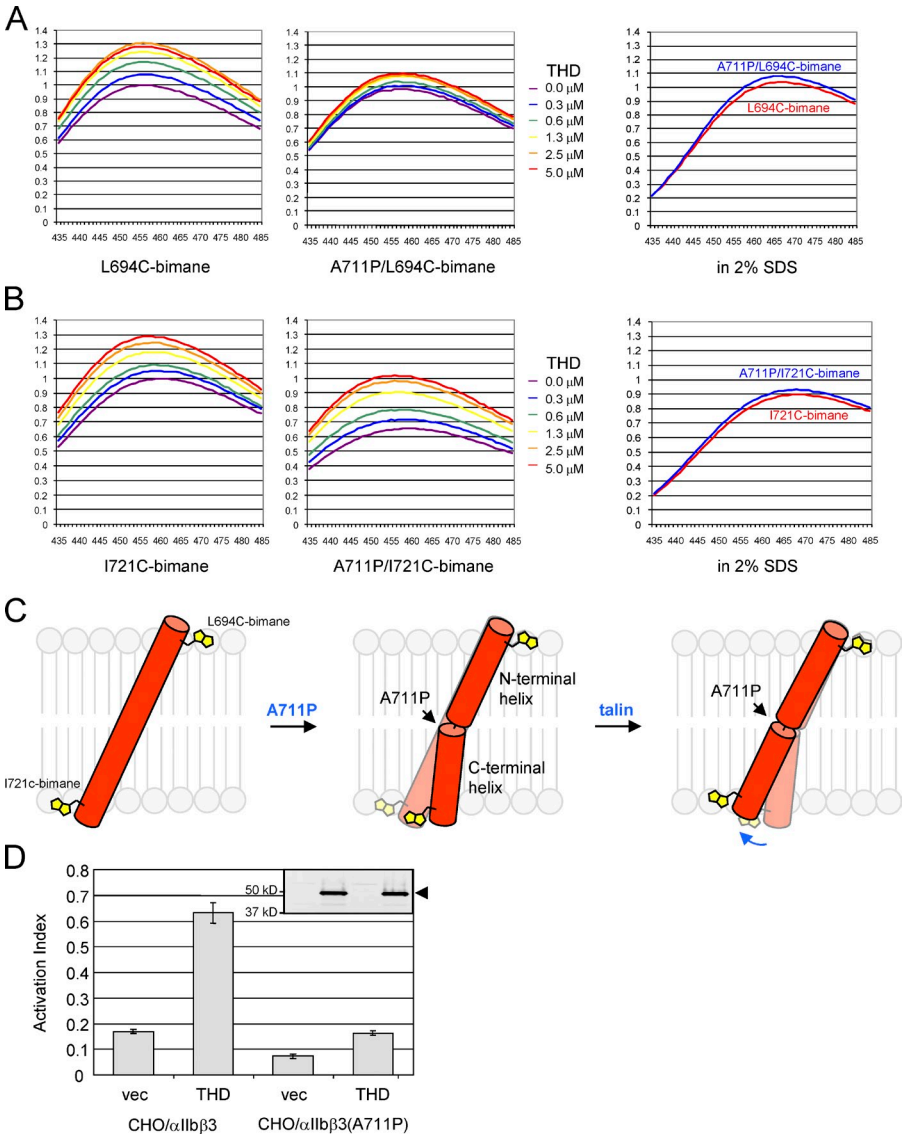

Figure 3. **A flexible kink in β3 TMD reduces transmission of talin-induced TMD topology change and integrin activation.** (A) Emission spectra of β3(L694C)-bimane nanodisc (left) in the presence of increasing concentrations of THD compared with those of β3(A711P,L694C)-bimane nanodisc (middle). Similar fluorescence intensities the in presence of 2% SDS are shown on the right. Fluorescence normalized to the maximum fluorescence intensity of L694C-bimane in the absence of talin is shown. (B) Emission spectra of β3(I721C) and β3(A711P,I721C)-bimane nanodiscs were analyzed as in A. (A and B) Data are representative of at least three independent experiments. (C) Effects of β3(A711P) mutation in response to THD. β3(A711P) breaks the TMD helix into two helices connected by a flexible kink; the flexible kink inhibits the transmission of THD-induced increased embedding across the membrane. (D) CHO cells stably expressing αIIbβ3 or αIIbβ3 (A711P) were transfected with THD or vector (vec), and αIIbβ3 activation was measured after 24 h. The arrowhead indicates the band corresponding to THD (~50 kD). Error bars are SEM of three independent experiments.

of L694C-bimane–labeled β3 (Fig. 3 A, middle). In sharp contrast, THD had similar effects on the fluorescence of β3 I721C-bimane in both the wild-type and A711P TMD tail constructs (Fig. 3 B, middle). Therefore, the Pro-mediated kink decoupled the N-terminal TMD helix from the THD-induced increased C-terminal helix embedding (Fig. 3 C, right). In consequence, the structural rigidity conferred by an unbroken helix is required to transmit the β3 TMD motion at the cytoplasmic face of the membrane to the extracellular face.

The integrin α and β TMD interact with each other to maintain integrins in an inactive state (Luo et al., 2004, 2005; Li et al., 2005; Partridge et al., 2005; Yin et al., 2007; Kim et al., 2009). Recent studies (Kim et al., 2011b) have confirmed the predicted importance of the TMD tilt angle in stabilizing this complex (Partridge et al., 2005). To test the hypothesis that talin might activate integrins by changing β3 TMD topology (Partridge et al., 2005; Wegener et al., 2007; Anthis et al., 2009; Kalli et al., 2010), we created an αIIbβ3(A711P) mutant and assessed its capacity to be activated by talin in cells. CHO cells stably expressing wild-type αIIbβ3 or αIIbβ3(A711P) were transfected with THD cDNA, and their binding to activation-specific PAC1 (Shattil et al., 1985) was assayed as described previously (Han et al., 2006). Expression of THD activated the wild-type integrin but failed to activate αIIbβ3(A711P) (Fig. 3 D). These results are consistent with the hypothesis that THDs induce β3 TMD topology changes at the inner membrane region, which is transmitted through a rigid β3 TMD to the outer membrane region. Thus, the capacity of talin to activate integrins depends on its ability to alter the topology of the entire β3 TMD.

Mechanism of talin-induced change in β3 membrane topology

To activate integrins, THD must interact with a membrane-proximal binding site on β3, which stabilizes the helical conformation of the β3 cytoplasmic tail (Fig. 4 A; Wegener et al., 2007; Anthis et al., 2009), thereby forming a rigid helix contiguous with the helical TMD. As structural rigidity is required to transmit talin-induced movement of the β3 cytoplasmic tail to the TMD, we reasoned that the talin-mediated TMD tilting might be dependent on this membrane-proximal β3–talin interaction.

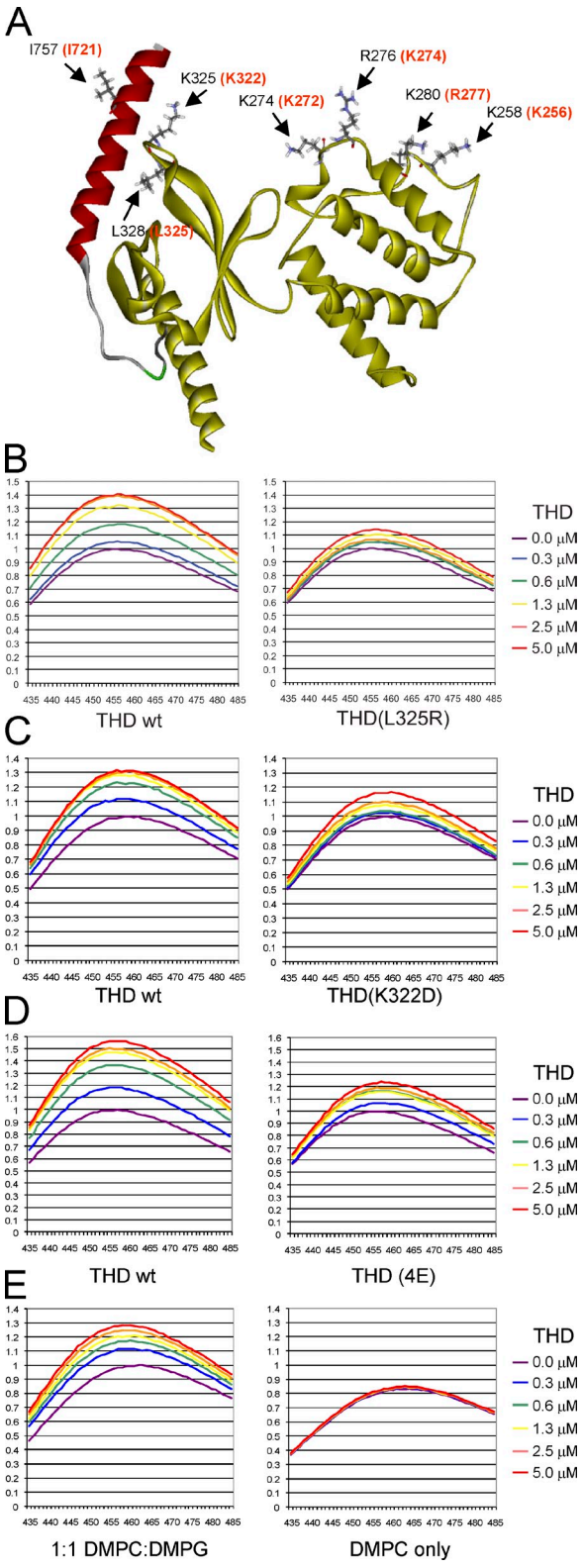

Figure 4. **Mechanism of talin-induced topology change.** (A) Crystal structure of talin2 F2-F3 (yellow) bound to integrin β1D tail (red; Protein Data Bank accession no. 3G9W). The amino acids in talin2 that bind to the membrane-proximal β1 tail (L328) and to lipid (K325, K258, K274, R276, and K280) are indicated with corresponding talin1 residues in parentheses. β1D(I757) (corresponds to β3(I721)), the position of bimane labeling, is indicated. (B) The emission spectra of L694C-bimane nanodiscs in the presence of increasing concentrations of THD (left) or THD(L325R) (right). wt, wild type. (C) Effect of THD(K322D), which blocks lipid binding, on the emission spectra was analyzed as in B. (D) Effect of mutations in lipid-binding residues of the THD F2 domain (K256E, K272E, K274E, and R277E) on the emission spectra was analyzed in as in B. (E) I721C-bimane nanodiscs were assembled with a 1:1 mixture of DMPC and DMPG (left) or with DMPC only (right), and their responses to the addition of THD were analyzed as in B. (B–E) Data are representative of at least three independent experiments.

A talin(L325R) mutation that disrupts this membrane-proximal interaction and inhibits integrin activation (Wegener et al., 2007) markedly attenuated the capacity of THD to alter the embedding of the β3 TMD (Fig. 4 B). Thus, the membrane-proximal β3–talin interaction is required for changing the embedding of the β3 TMD.

Talin-induced integrin activation requires that the integrin is membrane embedded (Ye et al., 2010) and the presence of lipid-binding basic residues in talin F3 (Wegener et al., 2007) and F2 (Anthis et al., 2009). Therefore, we asked whether the change in topology depends on the interaction between negatively charged phospholipids and basic residues on talin surface (Fig. 4 A). The increase in fluorescence intensity was reduced when THD proteins with acidic substitutions in lipid-binding basic residues in F3 (Fig. 4 C) or F2 (Fig. 4 D) domain were used. To examine the role of negatively charged phospholipids, we prepared neutral nanodiscs composed of zwitterionic lipid 1,2-dimyristoyl-*sn*-glycero-3-phosphocholine (DMPC). In contrast to the nanodiscs containing negatively charged 1,2-dimyristoyl-*sn*-glycero-3-phospho-(1'-rac-glycerol) (DMPG), THD failed to induce tilting in nanodiscs containing DMPC exclusively (Fig. 4 E). To ascertain that the topology change induced by THD is not a phenomenon limited to the particular model lipid, we created nanodiscs with negatively charged 1-palmitoyl-2-oleoyl-*sn*-glycero-3-phosphocholine/1-palmitoyl-2-oleoyl-*sn*-glycero-3-phospho-L-serine (POPC/POPS), in which the fatty acid chain length resembles that in platelet lipids (García-Guerra et al., 1996). THD induced an increase in fluorescence intensity of the bimane probe (Fig. S2 A), indicating a change of β3 TMD topology similar to that seen in DMPC/DMPG nanodiscs. Furthermore, this increase in fluorescence was abolished when we used THD(K322D-4E), in which lipid-binding basic residues in both F3 and F2 were mutated (Fig. S2 B). Thus, the interaction of THD with negatively charged membrane lipids is required for THD to alter the topology of the β3 TMD.

Kindlin-3 does not alter β3 TMD topology

As kindlins have been recently implicated in integrin activation (Kim et al., 2011a), we asked whether a kindlin has a similar effect on β3 TMD topology. Purified recombinant kindlin-3, the isoform involved in platelet αIIbβ3 activation, had no effect on fluorescence of bimane-labeled β3 TMD nanodiscs (Fig. S3). Furthermore, kindlin-3 did not augment the capacity of THD to induce the changes in bimane fluorescence (Fig. S3). Therefore, kindlin-3 did not induce changes in β3 TMD topology in this purified system.

Integrin α and β TMD interaction is required to maintain the low affinity state; these interactions are stabilized by inner and outer membrane clasps (Lau et al., 2009). The outer clasp

depends on specific packing interactions between α and β TMD and could thereby be disrupted by altering either TMD rotation or by decreasing or increasing the tilt angle of the β TMD. Indeed, β3(L716E) manifests a decreased tilt angle, destabilizes the α–β TMD interaction, and activates αIIbβ3 (Kim et al., 2011b). The effects of this decreased tilt angle are prevented by the flexible kink introduced by β3(A711P). Previous work suggested that talin could directly disrupt an α–β salt bridge that forms part of the inner clasp (Anthis et al., 2009); however, disrupting the salt bridge has a modest effect on the active–inactive conformational equilibrium because blocking talin binding reverses the activating effect of mutations that disrupt this salt bridge (Tadokoro et al., 2003; Wegener et al., 2007). The latter observation led to the suggestion that talin might also be able to disrupt the outer membrane clasp by binding to membrane phospholipids (Wegener et al., 2007; Anthis et al., 2009; Elliott et al., 2010), thereby creating an anchor point. The membrane-anchored talin was proposed to alter the rotation and/or tilt angle of the β TMD to disfavor the stability of the outer clasp; the thermodynamic validity of such a mechanism was supported by computational modeling (Kalli et al., 2010, 2011). The studies described here provide direct experimental proof that talin alters the membrane topology of the β3 TMD and that its capacity to do so requires that talin interacts with the β tail and negatively charged membrane lipids. We also show that the structural rigidity of the β TMD, which is broken by β3(A711P), is required to transmit talin-induced change in topology at the cytoplasmic face to the extracellular face and for talin to activate the integrin.

Integrin transmembrane signaling results from altered topology of a single-pass TMD. The importance of such changes in TMD topology have previously been demonstrated in multipass membrane proteins, such as G-protein–coupled receptors (Rosenbaum et al., 2009) and ion channels (Mayer, 2006). In these cases, multivalent ligand binding to multiple TMDs or sites physically connected to the TMDs displaces the TMDs relative to each other to change tilt angle. The talin-induced change in β TMD topology occurs with a single TMD; a lipid interaction provides a second anchor to enable talin to change the TMD topology in the absence of external force. Furthermore, negatively charged lipids were an important determinant in the THD-induced effect. Thus, talin-dependent integrin activation could be favored in membranes or in microdomains in which phosphatidyl serine or polyphosphatidyl inositol is abundant.

Materials and methods

Plasmids and reagents

A β3 TMD tail construct was prepared by ligation of the PCR-amplified β3 cytoplasmic tail region into a β3 TMD construct (Lau et al., 2008) in the pET-31 expression vector (EMD) with 6xHis and ketosteroid isomerase (KSI) tags as N-terminal fusions. Mutations on the β3 TMD tail construct such as L694C, I721C, K716E, and/or A711P were introduced by the QuikChange site-directed mutagenesis kit (Agilent Technologies). Monobromobimane was purchased from Sigma-Aldrich. Membrane scaffold protein MSP1D1 was provided by S. Sligar (University of Illinois, Chicago, IL). DMPC and DMPG were purchased from Avanti Polar Lipids, Inc. or Santa Cruz Biotechnology, Inc.

Expression and purification of integrin β3 TMD tail peptides

Escherichia coli BL21(DE3) transformed with β3 TMD tail constructs were grown at 37°C until they reached an OD_{600} of 1.0. 1 mM isopropyl thioglucose was added, and then cells were grown for 5 h at 37°C. Cells were harvested and lysed by sonication in lysis buffer (50 mM Tris-HCl, pH 7.4, 500 mM NaCl, 8 M urea, 20 mM imidazole, and 15 mM β-mercaptoethanol). The lysates were clarified by centrifugation. The clarified lysates were applied on a HiTrap Chelating HP column charged with Ni^{2+}. The column was washed twice with washing buffer I (lysis buffer without β-mercaptoethanol), resuspended with washing buffer I containing 1 mM monobromobimane, and incubated on a rocking plate under dark conditions at room temperature overnight. The column was washed twice with washing buffer II (50 mM Tris-HCl, pH 7.4, 500 mM NaCl, 6 M guanidine HCl, and 20 mM imidazole), and the labeled peptides were eluted with elution buffer (washing buffer II with 1 M imidazole). The Asp-Pro bond between KSI and β3 TMD tail peptide was cleaved in 10% formic acid for 120 min at 80°C (Lau et al., 2008), and 0.1% Triton X-100 was added to the eluate that was then dialyzed against 0.1% Triton X-100 in TBS (20 mM Tris-HCl, pH 7.4, and 150 mM NaCl). Precipitates consisting of KSI were removed by centrifugation at 14,000 rpm for 15 min, and solubilized β3 TMD tail peptides were concentrated to ∼10–20 µM (∼0.1–0.2 mg/ml) using Ultracel-10k (Millipore).

Preparation of nanodiscs

The preparation of nanodiscs was previously described (Ye et al., 2010). In brief, DMPC and DMPG lipids or POPC and POPS were dissolved in chloroform or chloroform/methanol mixture, mixed into a 1:1 ratio, and dried onto a glass tube with a steady flow of argon. The lipid mixture was dissolved in 100 mM cholate in TBS. To assemble nanodiscs, 360 µl of the 1:1 lipid mixture (50 mM), 1 ml of 200 µM MSP1D1 (provided by S. Sligar; Denisov et al., 2004), and the purified β3 TMD tail peptide (10 µM) were mixed. The mixture was added with 2 vol of Bio-Beads SM-2 (Bio-Rad Laboratories) to initiate nanodisc assembly and incubated overnight at room temperature in the dark. The assembled nanodiscs were further purified with a size-exclusion column (HiLoad 16/60 Superdex 200; GE Healthcare) with TBS as the column buffer. Fluorescence from each fraction was examined using a plate reader (Victor 2; PerkinElmer) and pooled according to the fluorescence profile and chromatogram. When necessary, the nanodiscs were further concentrated using Ultracel-30k (Millipore). Images of nanodiscs were taken on a microscope (Tecnai G2 Sphera; FEI) equipped with a 2k × 2k camera (Gatan, Inc.) at a magnification of 65,000× in DigitalMicrograph software (Gatan, Inc.).

Fluorescence spectroscopy

200 µl of the purified nanodiscs was mixed with 50 µl of various concentrations of either wild-type or mutant recombinant THD. After 20 min of incubation at room temperature, the emission spectrum (from 435 to 485 nm) at the excitation wavelength 370 nm was scanned with a 1-nm interval using a spectrofluorometer (FluoroMax-2; Instruments S.A., Inc.). The fluorescence from unlabeled β3 TMD tail peptide, talin, empty nanodisc, or buffer was negligible (<0.1% of signal from nanodiscs containing bimane-labeled β3 TMD tail peptide).

Cell lines and flow cytometry

Using a lentiviral cloning vector, pRRLSIN.cPPT.PGK-IRES-GFP.WPRE (plasmid ID 12252; Addgene), viruses containing αIIb or β3 gene were generated separately in 293T cells. CHO cells were infected with lentiviral particles containing human integrin αIIb by overnight incubation (Ye et al., 2010). The infected cells were then infected again with lentiviral particles containing either integrin β3 wild type or β3(A711P) to establish CHO/αIIbβ3 or CHO/αIIbβ3(A711P) cells. To test activating effects of THD on those integrins, 2 µg cDNA encoding THD and 0.1 µg cDNA encoding dTomato (as a transfection marker) were cotransfected. After 24 h, cells were detached, stained with PAC1 antibody followed by allophycocyanin-conjugated anti–mouse IgM antibody, and then analyzed by flow cytometry. Activation index was calculated as $(MFI - MFI_0)/(MFI_{max} - MFI_0)$, where MFI is the mean fluorescence intensity of PAC1 binding in transfected cells, MFI_0 is MFI in the presence of 20 µM eptifibatide, and MFI_{max} is MFI in the presence of anti-LIBS6 (Han et al., 2006).

Protein purification

C-terminal His6-tagged human THD and mutant were expressed in BL21-CodonPlus bacteria using pET30a vector and purified using Ni^{2+}–nitrilotriacetic acid beads, washed with 50 mM imidazole, and eluted with 500 mM imidazole (Ye et al., 2010). Kindlin-3 was expressed and purified from S2 insect cells. In brief, S2 insect cells stably expressing kindlin-3 with Flag and His6 purification tags were generated by selecting against blasticidin for 2 wk. Cells were cultured, harvested, and lysed

in TBS buffer (20 mM Tris and 150 mM NaCl, pH 7.4), and kindlin-3 was purified sequentially with Ni–nitrilotriacetic acid, anion exchange, and size-exclusion columns.

Online supplemental material

Fig. S1 shows that bimane fluorescence intensity increases when the hydrophobicity of the solvent increases. Fig. S2 shows that THD induces altered β3 TMD topology in POPC/POPS nanodiscs and that this effect of THD was completely abolished by mutations in F2 and F3 domains that block THD–lipid interactions. Fig. S3 shows that kindlin-3 neither induced nor synergized with THD in inducing β3 topology change. Online supplemental material is available at http://www.jcb.org/cgi/content/full/jcb.201112141/DC1.

Drs. Susan Taylor and Yuliang Ma (University of California, San Diego, La Jolla, CA) provided access to the spectrofluorometer, and Dr. Steven Sligar provided the membrane scaffold protein.

This work was supported by grants from the National Institutes of Health. C. Kim and F. Ye are postdoctoral fellows of the American Institute for Cancer Research and American Heart Association, respectively.

Author contributions: F. Ye, C. Kim, and M.H. Ginsberg conceived the project and wrote the manuscript. F. Ye, C. Kim, and X. Hu performed experiments.

Submitted: 27 December 2011
Accepted: 27 April 2012

References

Anthis, N.J., K.L. Wegener, F. Ye, C. Kim, B.T. Goult, E.D. Lowe, I. Vakonakis, N. Bate, D.R. Critchley, M.H. Ginsberg, and I.D. Campbell. 2009. The structure of an integrin/talin complex reveals the basis of inside-out signal transduction. *EMBO J.* 28:3623–3632. http://dx.doi.org/10.1038/emboj.2009.287

Cordes, F.S., J.N. Bright, and M.S. Sansom. 2002. Proline-induced distortions of transmembrane helices. *J. Mol. Biol.* 323:951–960. http://dx.doi.org/10.1016/S0022-2836(02)01006-9

Denisov, I.G., Y.V. Grinkova, A.A. Lazarides, and S.G. Sligar. 2004. Directed self-assembly of monodisperse phospholipid bilayer nanodiscs with controlled size. *J. Am. Chem. Soc.* 126:3477–3487. http://dx.doi.org/10.1021/ja0393574

Elliott, P.R., B.T. Goult, P.M. Kopp, N. Bate, J.G. Grossmann, G.C. Roberts, D.R. Critchley, and I.L. Barsukov. 2010. The structure of the talin head reveals a novel extended conformation of the FERM domain. *Structure*. 18:1289–1299. http://dx.doi.org/10.1016/j.str.2010.07.011

García-Guerra, R., J.A. García-Domínguez, and J. González-Rodríguez. 1996. A new look at the lipid composition of the plasma membrane of human blood platelets relative to the GPIIb/IIIa (integrin cxIIβ3) content. *Platelets*. 7:195–205. http://dx.doi.org/10.3109/09537109609023579

Ginsberg, M.H., A. Partridge, and S.J. Shattil. 2005. Integrin regulation. *Curr. Opin. Cell Biol.* 17:509–516. http://dx.doi.org/10.1016/j.ceb.2005.08.010

Han, J., C.J. Lim, N. Watanabe, A. Soriani, B. Ratnikov, D.A. Calderwood, W. Puzon-McLaughlin, E.M. Lafuente, V.A. Boussiotis, S.J. Shattil, and M.H. Ginsberg. 2006. Reconstructing and deconstructing agonist-induced activation of integrin alphaIIbbeta3. *Curr. Biol.* 16:1796–1806. http://dx.doi.org/10.1016/j.cub.2006.08.035

Hynes, R.O. 2002. Integrins: Bidirectional, allosteric signaling machines. *Cell*. 110:673–687. http://dx.doi.org/10.1016/S0092-8674(02)00971-6

Kalli, A.C., K.L. Wegener, B.T. Goult, N.J. Anthis, I.D. Campbell, and M.S. Sansom. 2010. The structure of the talin/integrin complex at a lipid bilayer: An NMR and MD simulation study. *Structure*. 18:1280–1288. http://dx.doi.org/10.1016/j.str.2010.07.012

Kalli, A.C., I.D. Campbell, and M.S. Sansom. 2011. Multiscale simulations suggest a mechanism for integrin inside-out activation. *Proc. Natl. Acad. Sci. USA*. 108:11890–11895. http://dx.doi.org/10.1073/pnas.1104505108

Kim, C., T.L. Lau, T.S. Ulmer, and M.H. Ginsberg. 2009. Interactions of platelet integrin alphaIIb and beta3 transmembrane domains in mammalian cell membranes and their role in integrin activation. *Blood*. 113:4747–4753. http://dx.doi.org/10.1182/blood-2008-10-186551

Kim, C., F. Ye, and M.H. Ginsberg. 2011a. Regulation of integrin activation. *Annu. Rev. Cell Dev. Biol.* 27:321–345. http://dx.doi.org/10.1146/annurev-cellbio-100109-104104

Kim, C., T. Schmidt, E.G. Cho, F. Ye, T.S. Ulmer, and M.H. Ginsberg. 2011b. Basic amino-acid side chains regulate transmembrane integrin signalling. *Nature*. 481:209–213. http://dx.doi.org/10.1038/nature10697

Kosower, N.S., E.M. Kosower, G.L. Newton, and H.M. Ranney. 1979. Bimane fluorescent labels: Labeling of normal human red cells under physiological conditions. *Proc. Natl. Acad. Sci. USA*. 76:3382–3386. http://dx.doi.org/10.1073/pnas.76.7.3382

Lau, T.L., A.W. Partridge, M.H. Ginsberg, and T.S. Ulmer. 2008. Structure of the integrin beta3 transmembrane segment in phospholipid bicelles and detergent micelles. *Biochemistry*. 47:4008–4016. http://dx.doi.org/10.1021/bi800107a

Lau, T.L., C. Kim, M.H. Ginsberg, and T.S. Ulmer. 2009. The structure of the integrin alphaIIbbeta3 transmembrane complex explains integrin transmembrane signalling. *EMBO J.* 28:1351–1361. http://dx.doi.org/10.1038/emboj.2009.63

Li, R., C.R. Babu, K. Valentine, J.D. Lear, A.J. Wand, J.S. Bennett, and W.F. DeGrado. 2002. Characterization of the monomeric form of the transmembrane and cytoplasmic domains of the integrin beta 3 subunit by NMR spectroscopy. *Biochemistry*. 41:15618–15624. http://dx.doi.org/10.1021/bi026822l

Li, W., D.G. Metcalf, R. Gorelik, R. Li, N. Mitra, V. Nanda, P.B. Law, J.D. Lear, W.F. Degrado, and J.S. Bennett. 2005. A push-pull mechanism for regulating integrin function. *Proc. Natl. Acad. Sci. USA*. 102:1424–1429. http://dx.doi.org/10.1073/pnas.0409334102

Luo, B.H., T.A. Springer, and J. Takagi. 2004. A specific interface between integrin transmembrane helices and affinity for ligand. *PLoS Biol.* 2:e153. http://dx.doi.org/10.1371/journal.pbio.0020153

Luo, B.H., C.V. Carman, J. Takagi, and T.A. Springer. 2005. Disrupting integrin transmembrane domain heterodimerization increases ligand binding affinity, not valency or clustering. *Proc. Natl. Acad. Sci. USA*. 102:3679–3684. http://dx.doi.org/10.1073/pnas.0409440102

Mayer, M.L. 2006. Glutamate receptors at atomic resolution. *Nature*. 440:456–462. http://dx.doi.org/10.1038/nature04709

Partridge, A.W., S. Liu, S. Kim, J.U. Bowie, and M.H. Ginsberg. 2005. Transmembrane domain helix packing stabilizes integrin alphaIIbbeta3 in the low affinity state. *J. Biol. Chem.* 280:7294–7300. http://dx.doi.org/10.1074/jbc.M412701200

Rosenbaum, D.M., S.G. Rasmussen, and B.K. Kobilka. 2009. The structure and function of G-protein-coupled receptors. *Nature*. 459:356–363. http://dx.doi.org/10.1038/nature08144

Sansom, M.S., and H. Weinstein. 2000. Hinges, swivels and switches: The role of prolines in signalling via transmembrane alpha-helices. *Trends Pharmacol. Sci.* 21:445–451. http://dx.doi.org/10.1016/S0165-6147(00)01553-4

Senes, A., D.E. Engel, and W.F. DeGrado. 2004. Folding of helical membrane proteins: The role of polar, GxxxG-like and proline motifs. *Curr. Opin. Struct. Biol.* 14:465–479. http://dx.doi.org/10.1016/j.sbi.2004.07.007

Shattil, S.J., J.A. Hoxie, M. Cunningham, and L.F. Brass. 1985. Changes in the platelet membrane glycoprotein IIb.IIIa complex during platelet activation. *J. Biol. Chem.* 260:11107–11114.

Shattil, S.J., C. Kim, and M.H. Ginsberg. 2010. The final steps of integrin activation: The end game. *Nat. Rev. Mol. Cell Biol.* 11:288–300. http://dx.doi.org/10.1038/nrm2871

Subczynski, W.K., R.N. Lewis, R.N. McElhaney, R.S. Hodges, J.S. Hyde, and A. Kusumi. 1998. Molecular organization and dynamics of 1-palmitoyl-2-oleoylphosphatidylcholine bilayers containing a transmembrane alpha-helical peptide. *Biochemistry*. 37:3156–3164. http://dx.doi.org/10.1021/bi972148+

Tadokoro, S., S.J. Shattil, K. Eto, V. Tai, R.C. Liddington, J.M. de Pereda, M.H. Ginsberg, and D.A. Calderwood. 2003. Talin binding to integrin beta tails: A final common step in integrin activation. *Science*. 302:103–106. http://dx.doi.org/10.1126/science.1086652

von Heijne, G., and D. Rees. 2008. Membranes: Reading between the lines. *Curr. Opin. Struct. Biol.* 18:403–405. http://dx.doi.org/10.1016/j.sbi.2008.06.003

Wegener, K.L., A.W. Partridge, J. Han, A.R. Pickford, R.C. Liddington, M.H. Ginsberg, and I.D. Campbell. 2007. Structural basis of integrin activation by talin. *Cell*. 128:171–182. http://dx.doi.org/10.1016/j.cell.2006.10.048

Williams, M.J., P.E. Hughes, T.E. O'Toole, and M.H. Ginsberg. 1994. The inner world of cell adhesion: Integrin cytoplasmic domains. *Trends Cell Biol.* 4:109–112. http://dx.doi.org/10.1016/0962-8924(94)90059-0

Yao, X., C. Parnot, X. Deupi, V.R. Ratnala, G. Swaminath, D. Farrens, and B. Kobilka. 2006. Coupling ligand structure to specific conformational switches in the beta2-adrenoceptor. *Nat. Chem. Biol.* 2:417–422. http://dx.doi.org/10.1038/nchembio801

Ye, F., G. Hu, D. Taylor, B. Ratnikov, A.A. Bobkov, M.A. McLean, S.G. Sligar, K.A. Taylor, and M.H. Ginsberg. 2010. Recreation of the terminal events in physiological integrin activation. *J. Cell Biol.* 188:157–173. http://dx.doi.org/10.1083/jcb.200908045

Yin, H., J.S. Slusky, B.W. Berger, R.S. Walters, G. Vilaire, R.I. Litvinov, J.D. Lear, G.A. Caputo, J.S. Bennett, and W.F. DeGrado. 2007. Computational design of peptides that target transmembrane helices. *Science*. 315:1817–1822. http://dx.doi.org/10.1126/science.1136782